Ornamental Horticulture
ISSN 2447-536X | WWW.ORNAMENTALHORTICULTURE.COM.BR
SBFPO Sociedade Brasileira de Floricultura e Plantas Ornamentais

ARTICLE

The androecium of *Adenium obesum* (Apocynaceae): anther and pollen grains development

O androceu de *Adenium obesum* (Apocynaceae): desenvolvimento da antera e dos grãos de pólen

Deborah Cristina Dias Campos[1], Clivia Carolina Fiorilo Possobom[1], Elka Fabiana Aparecida Almeida[1], Sabrina Maihave Barbosa Ramos[1], and Silvia Nietsche[1,*]

[1]Universidade Federal de Minas Gerais, Instituto de Ciências Agrárias, Montes Claros-MG, Brasil

Abstract: In this study, we describe anther development in *Adenium obesum*, providing information on microsporogenesis, microgametogenesis, and the structure of mature pollen grains. Buds and flowers at various developmental stages were collected from cultivated plants of an accession characterized by a simple, pink corolla. The samples were processed following standard protocols for light microcopy analysis, including histochemical tests, to identify starch and lipids. The androecium of *A. obesum* comprises five epipetalous stamens with anthers arranged in a conical structure that covers the apex of the style. The stamens are adnate to the petals through short filaments and are connected to the style head through unicellular trichomes, forming the gynostegium. The anthers are dithecous, tetrasporangiate, and longitudinally dehiscent. The development of parietal layers follows the dicotyledonous pattern, with the mature anther wall comprising an epidermis, endothecium, two to three middle layers, and secretory tapetum. The tetrads exhibit a tetrahedral arrangement, and cell division is of the simultaneous type. The pollen grains are bicellular, contain starch reserves, and are dispersed as monads, held together by a lipophilic substance. In the access studied here, no evidence of male sterility was observed. The main events during anther and pollen grain development in *A. obesum* were categorized as pre-meiotic, meiotic, and post-meiotic, and were correlated with the collection stages examined in this study. Our results provide morphological markers for these processes and can aid in implementing *in vintro* anther or microspore culture techniques, which are promising alternatives for the genetic improvement of the species.
Keywords: anatomy, desert rose, microgametogenesis, microsporogenesis.

Resumo: O presente trabalho descreve o desenvolvimento das anteras em *Adenium obesum*, fornecendo informações sobre microsporogênese, microgametogênese e a estrutura dos grãos de pólen maduros. Botões e flores em diferentes estádios de desenvolvimento foram coletados de plantas cultivadas pertencentes a um acesso caracterizado pela corola simples e coloração rosa. As amostras foram processadas seguindo protocolos convencionais para analise sob microscopia óptica, incluindo testes histoquímicos para identificação de amido e lipídios. O androceu de *A. obesum* é compoto por cinco estames epipétalos cujas anteras se organizam em uma estrutura cônica que recobre o ápice do estilete. Os estames são adnatos às pétalas através do filete curto e são conectados à cabeça do estilete através de tricomas unicelulares que formam o ginostégio. As anteras são bitecas, tetraesporangiadas e apresentam deiscência longitudinal. O desenvolvimento dos estratos parietais segue o padrão dicotiledôneo, sendo a parede da antera madura constituída por epiderme, endotécio, duas a três camadas médias e tapete secretor. As tétrades apresentam arranjo tetraédrico e a divisão celular é do tipo simultânea. Os grãos de pólen são bicelulares, contêm reserva amilácea e são dispersos em mônades, agrupados por substância lipofílica. No acesso analisado, não foram observadas evidências de esterilidade masculina. Os principais eventos do desenvolvimento das anteras e dos grãos de pólen de *A. obesum* foram classificados em pré-meióticos, meióticos e pós-meióticos e relacionados com os estádios de coleta aqui considerados. Os resultados obtidos permitiram o estabelecimento de marcadores morfológicos desses processos, podendo subsidiar a implementação de técnicas de cultura *in vitro* de anteras ou de micrósporos, alternativas promissoras para o melhoramento genético da espécie.
Palavras-chave: anatomia, microgametogênese, microsporogênese, rosa-do-deserto.

Introduction

Adenium obesum (Forssk.) Roem. & Schult., commonly known as Desert Rose, is a succulent plant native to sub-Saharan Africa and the Arabian Peninsula, highly valued for its ornamental qualities (Santos et al., 2020). Belonging to the Apocynaceae, to the informal rank Apocynoid and the tribe Nerieae (Endress et al., 2018), this species is a shrub with a swollen main stem at the base, forming a broad caudex. It has simple leaves arranged spirally and clustered at branch apices, where showy flowers appear in thyrsoid inflorescences (Possobom et al., 2021).

Apocynaceae flowers are referred to as complex, mainly based on their high synorganization, with congenital and postgenital fusion of floral organs, especially in relation to androecium and gynoecium (Endress et al., 2016 and references therein). The most extremely complex flowers had corona, gynostegium and pollinarium, being the former formed by corolla and androecium fusion and the last two formed by the fusion of androecium and gynoecium. (Endress et al., 2016). Apocynoideae representatives, like *A. obesum*, are characterized by a corolla with dextrorse aestivation; lignified anthers that are fertile in the upper part, with the lower portion adnate to the style head, forming the gynostegium; pollen grains arranged in monads or tetrads; follicular fruits; and comose seeds (Endress and Bruyns, 2000).

Although the flowers of *A. obesum* exhibit the general floral architecture typical of the taxonomic group, they can vary in terms of size, longevity, number, coloration, and morphology of the petals; stamen length, which may be included or exserted; morphology of the staminal appendages; number of fertile stamens; presence and number of petaloid or secretory staminodes; pollen grain viability; and morphology of the style head (Plaizier, 1980; Hastuti et al., 2009; Colombo et al., 2018; Singh et al., 2019; Possobom et al., 2021; Ramos et al., 2022). This great morphological and functional variation in flowers highlights the wide genetic diversity associated with this species and underscores the importance of expanding the documentation of this variability to support and guide genetic improvement programs.

Colombo et al. (2018) stated that all commercially available *Adenium* spp. are hybrids and exhibit high genetic variation when grown from seeds. Vegetative propagation is preferred when maintaining the characteristics of cultivars, with cuttings and grafting being the primary techniques used (Colombo et al., 2018; Nunes and Pereira, 2021). However, plants

*Corresponding author: snietsche@ufmg.br | https://doi.org/10.1590/2447-536X.v31.e312836 | Editor: Margherita Beruto, Coordenadora da Divisão de Plantas Ornamentais da ISHS, Italy | Received: Oct 29, 2024 | Accepted: Apr 18, 2025 | Available online: June 16, 2025 |

propagated vegetatively often lack the well-shaped caudex found in seed-propagated plants (Colombo et al., 2015; Colombo et al., 2018; Santos et al., 2015), potentially reducing the commercial value of the seedlings.

The seed propagation of *A. obesum*, a predominantly allogamous species, relies on successful cross-pollination, which is artificially achieved in cultivated plants but can be hindered by the floral complexity, morphological variability, and male or female sterility (Possobom et al., 2021, Ramos et al., 2022).

Pollen grain development is a crucial process in plant reproduction, as pollen is directly responsible for fertilization and various factors during the anther wall formation, microsporogenesis or microgametogenesis can interfere with proper pollen formation, potentially leading to male sterility, as has already been reported for other angiosperm species, including some Apocynaceae (Laser and Lersten, 1972; Bhandari, 1984; Sud, 1984; Chaban et al., 2020).

In angiosperms, developmental abnormalities can be observed before or after meiosis: during the formation of sporogenic tissue, after microspore release, or during male gametophyte development (Laser and Lersten, 1972; Bhandari, 1984, Sud, 1984; Chaban et al., 2020). Changes in anther development have also been reported, including atrophy or fusion of pollen sacs (Chaban et al., 2020), and alterations in tapetum functionality, which is responsible for releasing various compounds essential for microspore (Laser and Lersten, 1972; Bhandari, 1984; Sud, 1984; Chaban et al., 2020).

Furthermore, understanding processes, such as microsporogenesis and microgametogenesis, is crucial for implementing in-vitro anther or microspore culture techniques, which are used to develop double haploid plants, thereby reducing the time required to produce homozygous strains (Seguí-Simarro, 2021). These techniques offer an alternative approach for improving *A. obesum*, which is one of the goals of our research group.

Knowledge regarding anther and pollen grain morphology and development is not only economically important but also taxonomically relevant for establishing patterns within the Apocynaceae (Endress et al., 2014; Fishbein et al., 2018; Souza et al., 2022). This information remains limited or unavailable for many taxa, including *A. obesum,* but could be relevant for understanding the diversity of the androecium and pollen development in Apocynaceae, contributing to a better understanding of evolutionary aspects within the family (Alves et al., 2025).

Additionally, in a previous study with three accessions of *A. obesum* - ICA-ps (purple, simple), ICA-wd (white, double), and ICA-rt (red, triple) - cultivated at the Institute of Agricultural Sciences (ICA), Federal University of Minas Gerais (UFMG), Ramos et al. (2022) reported a wide variation in the androecium, which exhibited different types and degrees of male sterility. They recorded the presence of anthers with variable amounts of unviable or deformed pollen grains (pollen sterility), as well as stamens modified into petaloid or secretory staminodes (structural sterility).

Considering the economic potential of *A. obesum*, lack of basic information on its floral development, and importance of this knowledge for improving propagation techniques and genetic programs, as well as contributing to the family's systematics, in this study, we aimed to characterized the morphology and development of the androecium in an *A. obesum* accession cultivated in ICA/UFMG. We focused on the (1) anther wall layers development, and (2) microsporogenesis and microgametogenesis processes.

Material and Methods

Plant material and growing conditions

We used 60 plants from an *A. obesum* accession characterized by its simple, pink corolla (ICA-pks, Fig. 1A). The plants were grown in 4-L pots filled with commercial substrate (Bioplant®) and placed on 1-m-high benches in a greenhouse at the Institute of Agricultural Sciences (ICA) of the Federal University of Minas Gerais (UFMG), Montes Claros Campus, Montes Claros, Minas Gerais, Brazil (16.6856° S, 43.8469° W). The pots were watered weekly and fertilized with a solution of 10 g of Fort flores® commercial fertilizer dissolved in 2 L of water and applied to the substrate surface.

Collections were conducted randomly within the population throughout 2020, with the highest availability of reproductive material occurring between April and July. Samples of floral buds and flowers at various developmental stages were collected and processed for light microscopy analysis.

Light microscopy analysis

Samples of floral buds and flowers were categorized into ten developmental stages based on their morphological characteristics, besides length and maximum diameter (Fig. 1B-1D, Table 1). At least three samples from each stage were fixed in FAA 70 solution for 48 hours (Johansen, 1940) and preserved in 70% ethanol for subsequent processing and analysis at the Microscopy, Microanalysis and Plant Biology laboratory of the Institute of Agricultural Sciences, UFMG.

Pieces of anthers from all the developmental stages (Table 1) were dehydrated using an ethanolic series (80%, 90%, 99.5%), infiltrated and embedded in glycol methacrylate resin (Historesin, Leica®) according to the manufacturer's recommendations. Longitudinal and transverse sections, with thickness of 4 μm, were obtained using a rotary microtome (Yidi-YD-315). The sections were stained with 0.05% toluidine blue at a pH of 4.7 (O'Brien et al., 1964) and mounted with coverslips using Acrilex® vitreous varnish.

Anthers from pre-anthesis buds and flowers at anthesis were subjected to histochemical tests using Lugol's reagent and Sudan III to detect starch and lipids, respectively (Johansen, 1940).

The slides were analyzed and photo-documented using a light microscope (Primo Star Zeiss) equipped with a digital camera.

Fig. 1. Plant material of *Adenium obesum* (acessium ICA-pks). **A**. Cultivated individual showing the caudex, leaves and a newly opened flower. **B.** Early stages of the inflorescence development. **C.** Inflorescence with various developmental stages. **D.** Developmental stages examined in this study.

Table 1. Characterization of the developmental stages of floral buds and flowers of *Adenium obesum* examined in this study.

Stages	Length (cm)	Maximum diameter (cm)	Description
1	< 0.5	< 0.1	Very young floral buds fully covered by sepals and bracts, occuring in clusters at the early stages of inflorescence development. Anthers approximately 0.4 mm in diameter.
2	0.5 to 0.6	0.1	Young buds, fully covered by sepals, more elongated and individualized than stage 1. Anthers approximately 0.6 mm in diameter.
3	0.6 to 1.0	0.15	Buds with corolla lobes visible, exhibiting dextrorse aestivation. Sepals covering approximately 2/3 of the length. Anthers approximately 0.8 mm in diameter.
4	1.0 to 1.5	0.19	More elongated buds, sepals covering approximately 3/5 of the length.
5	1.5 to 2.0	0.27	Buds with part of the floral tube visible, sepals covering approximately 1/2 of the length.
6	2.0 to 2.8	0.36	Buds with sepals covering approximately 1/4 of the length.
7	2.8 to 4.5	0.51	Buds with a longer floral tube, sepals covering approximately 1/5 of the length.
8	4.5 to 5.0	0.58	Buds with sepals covering approximately 1/6 of the length.
9	5.0 to 5.4	0.74	Buds with loose petals, sepals covering only the narrow part of the floral tube (approximately 1/7 of the length). Anthers approximately 1 mm in diameter.
10	5.4 to 6.8	0.85	Flowers at anthesis, sepals partially covering the narrow part of the floral tube.

Results

General characterization of the androecium

The androecium of *A. obesum* (acessium ICA-pks) comprises five epipetalous and exserted stamens densely covered by non-glandular trichomes along their entire length, each approximately 4 cm long in the flowers at anthesis (Fig. 2A). The filaments are short, sturdy and greenish, attached at their base to the petals where the narrow part of the floral tube widens. The basifixed, bithecae and longitudinally dehiscent anthers are juxtaposed, forming a cone-shaped structure that completely covers the style head (Fig. 2A-2B). They are triangular with a sagittal base, featuring two non-fertile wings, and have an apex with long, filiform appendages that are reddish and twisted at the ends (Fig. 2A).

Floral bud samples, which were analyzed in their entirety, revealed unicellular trichomes on the ventral epidermis of the filament in contact or intermingled with trichomes on the epidermis of the style head (Fig. 2B-2C). This represents some degree of fusion between the two reproductive whorls - the androecium and gynoecium - characterizing the gynostegium. This structure was not observed in later developmental stages, because only the anthers were individually analyzed.

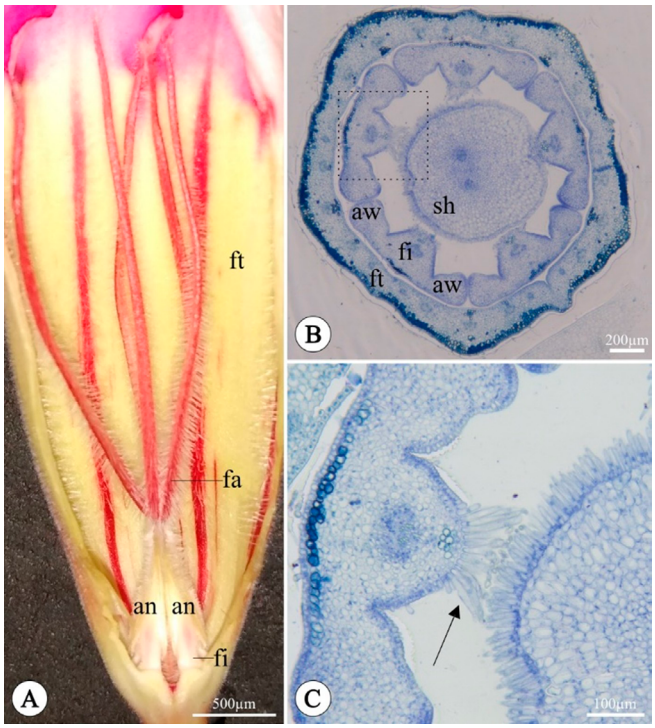

Fig. 2. General characterization of the androecium in *Adenium obesum*. **A.** Longitudinal section of an entire flower, showing the filaments (fi), anthers (an) and filiform appendages (fa) inside the wider part of floral tube (ft). **B.** Cross section of floral bud at the level of the filament (fi) insertion. Note the floral tube (ft) and the juxtaposition of the anther wings (aw) around the style head (sh). **C.** Detail of the dotted retangle in the figure B, showing the unicellular trichomes connecting the filament's ventral region to the style head (gynostegium).

Anther wall development

In young buds (stage 1) approximately 1 mm in diameter, longitudinal sections revealed that the calyx, corolla, androecium, and gynoecium were already distinct structures (Fig. 3A). The sepals were more developed than the other whorls. At this stage, the stamens were approximately 0.8 mm long and sickle-shaped, with minimal differentiation among the filament, anther, and filiform appendage (Fig. 3A). Cross-sections of young anthers from the same stage were approximately 0.4 mm wide and had a slight four-lobed shape (Fig. 3B). The anthers were tetrasporangiate and constituted by the protoderm, fundamental meristem and a central procambial bundle. Below the protoderm in the lobe region, a layer of organized, juxtaposed cells was visible. These cells have a quadrangular shape, dense cytoplasm, and large nuclei, forming the primary parietal layer (Fig. 3B-3D). Deeper inside, the sporogenic tissue is distinguishable by its larger cells (Fig. 3B-3E), some of them showing evidence of mitotic division (Fig. 3D). Periclinal divisions in cells of the primary parietal layer give rise to the inner and outer secondary parietal layers (Fig. 3E). Concurrently, newly divided cells of the outer secondary parietal layer are visible (Fig. 3D). Cells derived from the outer secondary periclinal division form the endothecium and middle layers, whereas the inner secondary parietal layer differentiates into the tapetum.

Anthers from flower buds at stage 2 were approximately 0.6 mm wide, with four distinct lobes, each containing a differentiated microsporangium (Fig. 3F). A pronounced groove is visible ventrally between the thecae. Dorsally, in the connective region, there is a uniseriate epidermis, a layer of subepidermal cells containing phenolic compounds in their vacuoles, several layers of isodiametric cells with peripheral cytoplasm, well-developed vacuoles, and prominent nuclei. A centrally positioned vascular bundle with a few fully differentiated vessel elements is also present (Fig. 3F). The parietal layers lining each microsporangium are fully formed, comprising one epidermal layer, one endothecial layer, two to three middle layers, and one tapetal layer (Fig. 3F-3G).

The epidermal cells are small and range from cuboidal to rectangular in shape. They have thin walls and a thin cuticle, well-developed vacuoles, and distinct nuclei located at the base of the cells. The cells of the endothecium are more voluminous than the cells of the middle layer, but are similar, rectangular, and periclinally flattened. They have thin walls, large vacuoles, and clear nuclei located at the periphery. The tapetal cells are large, irregularly shaped, and have thin walls. They contain dense, abundant cytoplasm, a small vacuole, and a large nucleus (Figs. 3F-3G).

From stage 3 onward, the samples possessed anthers with diameters exceeding 0.8 mm. These anthers began to show a groove in the septal region between microsporangia of the same theca, corresponding to the stomium area (Fig. 3H).

As the anthers matured, changes in shape, volume, cytoplasm, and cell wall characteristics were observed in the cells comprising the various parietal layers (Fig. 3H-3I).

The epidermal cells showed slightly thicker walls and cuticle, a large vacuole, peripheral cytoplasm, and a less prominent nucleus (Fig. 3I). The endothecium cells became quadrangular and larger. From stage 7 onward, they developed fibrillar thickenings in their walls (Fig. 3I-3J). These thickenings occur in the cells surrounding the microsporangia, with more than one cell layer present in certain regions, particularly near the connective tissue (Fig. 3I). In these areas, it is possible that cells other than the endothecial ones—such as persitent middle layer cells—also develop wall thickenings. The cells in the middle layers are rectangular, larger, and highly vacuolated, and almost all of them disappear even before the microsporangium is ready to dehisce. The tapetal cells showed increased vacuolation and underwent degradation as the microspore development advanced. From stage 4 onward, the tapetal cells were no longer visible, having been completely degraded.

In samples collected from pre-anthesis buds (stage 9), the anthers were approximately 1 mm wide and showed a ruptured stomium in the septal region between two microsporangia (Fig. 3I). The epidermis and endothecium were the only intact layers of the parietal strata as the cells of the middle layers in this region collapsed.

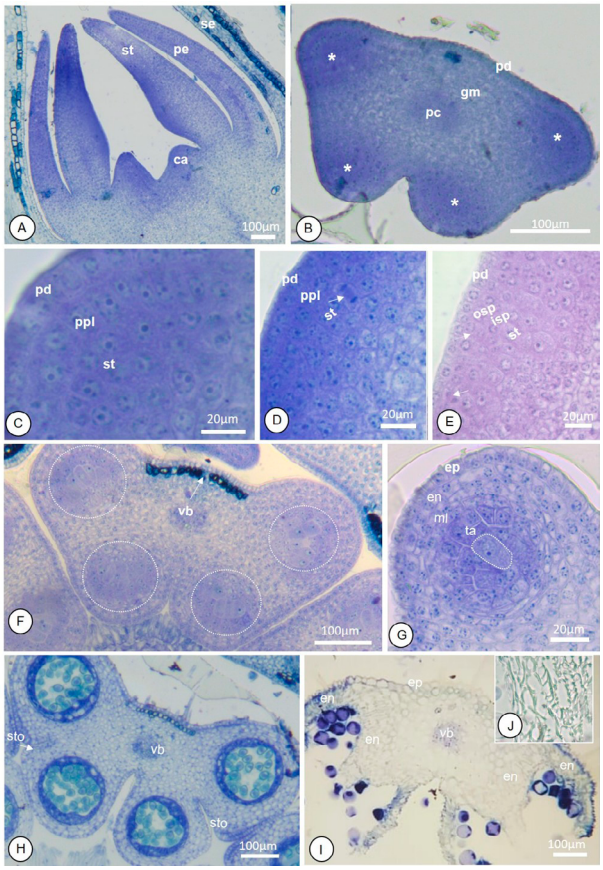

Fig. 3. Anther parietal layers development in *Adenium obesum*. Longitudinal (**A**, **D**, **E,** and **J**) and transverse (**B**, **C**, **F**, **G**, **H**, and **I**) sections stained with toluidine blue. **A.** A flower bud in early development showing sepals (se) at a more advanced stage of differentiation and morphogenesis than the other parts: petals (pe), stamens (st), and carpels (ca). Notably, the sickle-shaped stamens show minimal differentiation between their parts. **B.** A young anther with a tetralobate shape, featuring a protoderm (pd), a connective with ground meristem (gm), central procambial bundle (pc) and four undifferentiated microscporangia (*) **C.** Detail of a microsporangium showing protoderm (pd), primary parietal layer (ppl), and sporogenous tissue (st). **D.** Periclinal division of the sporogenous tissue (st) secondary wall. **E**. Detail showing protoderm (pd), outer secondary parietal layer (osp), inner secondary parietal layer (isp), and sporogenic tissue (st). The arrows indicate cell division in the outer parietal layer to form the endothecium and middle layer. **F.** Anther showing four microsporangia (dotted circle) and the vascular bundle (vb). The arrow indicates the subepidermal cells with phenolic content. **G.** Detail of anther showing epidermis (ep), endothecium (en), middle layer (ml), secretory tapetum (ta) and outlined microspore mother cell. **H.** Anther showing the stomium region (sto). **I.** Mature anther after dehiscence and mature pollen grains releasing. Note the endothecial cells (en). **J.** Detail showing the fibrous thickenings of the endothecial cells walls.

Microsporogenesis and microgametogenesis

Inside the microsporangia, cells of the sporogenous tissue undergo mitotic division (Fig. 3E), producing microspore mother cells. These cells are visible in samples collected from buds at stage 2 (Figs. 3F-3G and 4A-4B).

In the cross-section, these cells are organized in rows connected by their longest walls. They are rectangular and large, with a dense, abundant cytoplasm, small vacuole, and large, centrally located nucleus (Figs. 3F, 3G, 4A, and 4B). At this stage, some samples revealed the onset of callose deposition, visible as a thin transparent layer surrounding each microspore mother cell (Fig. 4B). In some samples, these cells were observed undergoing meiosis, initially producing two (Fig. 4C) and subsequently four haploid cells (Fig. 4D), resulting in tetrads in tetrahedral arrangement. After the dissolution of the callose, the four microspores are released. In some samples, they can be seen close together, still exhibiting a tetrahedral arrangement (Fig. 4E).

From stage 3 onward, the microspores are completely separated (Fig. 4F), revealing their irregular outlines and newly formed exine. Simultaneously, an enlargement of the vacuole can be observed, whereas the cytoplasm and nucleus remain in a peripheral position.

Each microspore undergoes asymmetrical mitosis, producing two cells: larger vegetative and smaller generative cells (Fig. 4G). This process forms the young microgametophyte.

From stage 5 (Fig. 4H-4I), mature pollen grains are visible, having adopted a circular shape. Although detailed analyses of pollen grains typically require acetolysis techniques or scanning electron microscopy, the conventional light microscopy employed in the present study enabled the observation of specific structural features of *A. obesum* pollen grains, they are primarily tricolpate, with an apparently smooth exine and thin intine, except near the openings where the intine thickens. The cells have a dense, abundant cytoplasm. The nucleus of the vegetative cell is larger than the ellipsoid-shaped nucleus of the generative cell (Fig. 4H-I). In the dispersal stage, the pollen grains of *A. obesum* are bicellular and released as monads.

Histochemical tests revealed lipophilic droplets in the parietal strata cells of the anther, particularly in the tapetum, when microspores are free (Fig. 5A). We did not observe lipophilic substances inside microspores (Fig. 5A) or mature pollen grains in the dispersal stage (Fig. 5B). However, a lipophilic substance was observed surrounding and binding pollen grains together in a mass in the dispersal stage (Fig. 5B). Starch grains were present in both free microspores and mature pollen grains (Fig. 5C-5D).

Table 2 presents the main events during androecium development in *A. obesum*, which were categorized as pre-meiotic, meiotic, and post-meiotic, corresponding to the collection stages examined in this study (Table 1).

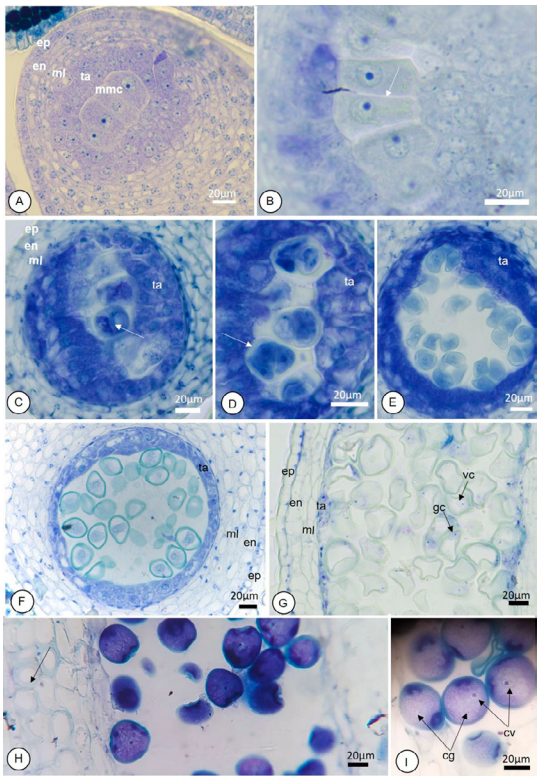

Fig. 4. Microsporogenesis and microgametogenesis in *Adenium obesum*. Cross - (**A**, **B**, **D**, and **E**) and longitudinal sections (**F**, **G**, and **H**). **A.** Microspore mother cells (mmc). **B.** Detail of the microspore mother cells. The arrow indicates the beginning of callose deposition. **C.** End of meiosis II; the four haploid nuclei are still joined by a single wall containing callose (arrow). **D.** Newly individualized microspores with a tetrahedral arrangement (arrow). **E.** Free microspores. Notably, the vacuoles in the microspores and tapetal cells (ta) have increased, and the exine is already deposited. **F-G.** Vacuolization. The tapetum (ta) is almost completely degenerated and the middle layers are still present. Pollen grains with two nuclei after mitosis: generative (gc) and vegetative cells (vc). **H-I.** Mature pollen grain; showing the generative (gc) and vegetative cells (vc). In H, the arrow indicates the thickening of the endothecial cells walls. en: endothecium, ep: epidermis, ml: middle layer, ta: tapetum.

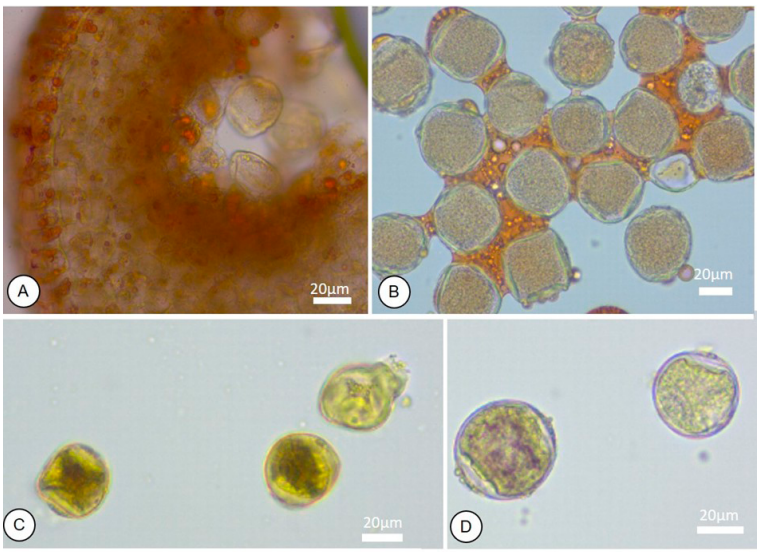

Fig. 5. Histochemical tests on *Adenium obesum* with Sudan III (**A, B**) and Lugol **(C-D***)*. **A**. Cross-section of the anther at stage 4. The positive reaction in the cells of the parietal layers is evident, especially in the tapetum. **B-D.** Mature pollen grains. Note lipophilic substance surrounding the pollen grains (**B**) and small starch grains inside then.

Table 2. Pre-meiotic, meiotic, and post-meiotic events observed during anther and pollen grain development in *Adenium obesum*, and their correlation with the collection stages examined in this study.

	Collection stages	Events
Pre-meiosis	1	Cells of the primary parietal layer divide periclinally to form the inner and outer secondary parietal layers. The outer secondary parietal layers divide periclinally to form the endothecium and middle layers, whereas the inner secondary parietal layer forms the tapetum. The sporogenous tissue divides to produce the microspore mother cells.
Meiosis	2	Microsporangia are evident, parietal strata are formed, and microspore mother cells are visible. Callose is deposited around the microspore mother cells. Tapetal cells undergo vacuolization. Meiosis and microspore formation occur (simultaneous cytokinesis/tetrahedral tetrads).
Post-meiosis	3	Stomata are formed in the area between microsporangia of the same thecae. Free microspores are observed (end of microsporogenesis). Vacuolization of microspores occurs. Asymmetric mitotic division occurs and result in the formation of vegetative and generative cells (microgametogenesis). The tapetum begins to deteriorate.
	4	The tapetum is totally degraded.
	5-8	A young microgametophyte is formed. Thickening occurs in the endothecial walls.
	9	Anther dehiscence.
	10	Three-celled, bicellular pollen grains with starch reserves are observed; they are dispersed as monads, joined by a lipophilic substance (pollenkitt) to form a mass.

Discussion

The androecium of the investigated plants shares similar characteristics with those previously reported for other accessions of *A. obesum* (Ramos et al., 2022) and other Apocynoids (Fallen, 1986; Endress and Bruyn, 2000; Endress et al., 2018). Contrary to the findings of Ramos et al. (2022), our results showed no evidence of male sterility in accession ICA-pks.

The presence of a gynostegium is a common characteristic among members of the Apocynaceae family and is important for understanding its systematics and pollination mechanisms (Fishbein et al., 2018; Perez-Lopes et al., 2023). This structure is characterized by varying degrees of post-genital fusion between the gynoecium and androecium parts, which guide pollinators for efficient pollen transfer (Fishbein et al., 2018). The anthers of *A. obesum* are separate and mostly detached from the style cells, except in the ventral filament region, where long adjacent trichomes, which closely contacts the epidermal cells of the style head. This structure represents a synorganization of these whorls, forming a gynostegium, similar to that reported for some species of *Secondatia* (Simões et al., 2007), with the same functional importance as structures with higher degrees of adnation between these whorls.

The anthers of *A. obesum* are tetrasporangiate, a characteristic common to most members of the Apocynaceae family, except for the Asclepiadoideae subfamily, which may have bisporangiate anthers (Endress and Bruyns, 2000; Solomon Raju et al., 2021). A similar pattern has been reported for other genera in this family, including *Rauvolfia* (Koch et al., 2018) and *Aspidosperma* (Alves et al., 2025).

Similarly, the development of parietal layers in the anthers of *A. obesum* follows the dicotyledonous pattern as the outer secondary parietal layer cells divide periclinally, forming the endothecium and middle layer cells. The inner secondary parietal layer cells, in turn, form the tapetal cells. This aligns with the results of other Apocynaceae species (Koch et al., 2018; Alves et al., 2025).

The number of layers in the anther wall can vary both between and within species. Alves et al. (2024) suggest that the number of parietal layers in anthers has increased in more recently evolved groups. Five to six layers were observed in *A. obesum*, wherein the number of middle layers varied. We identified distinct stages of intense cell division, which contribute to the formation of various layers in the anther wall and development of pollen grains in mature anthers. We also revealed stages where cells expand and differentiate, acquiring characteristics essential for the full functionality of the male reproductive structure. These transformations provide important records of the dynamic functioning of the androecium.

Analysis of *A. obesum* material indicates that most cells comprising the anther's parietal layers form considerably early in flower buds measuring up to 0.6 cm in length and 0.1 cm in diameter. After this stage, the anthers undergo gradual increases in size, with widths ranging from approximately 0.4 mm at stage 2 to 1 mm at stage 9. These variations result from the expansion and differentiation of previously formed cells.

Among the parietal layers, the endothecium functions as mechanical tissue during anther dehiscence owing to parietal thickening. In *A. obesum*, these cells have thickened fibrillar walls, a common feature in the Apocynaceae family and other families of the Gentianales order (Carrillo-Ocampo et al., 2023). *Rauvolfia* (Koch et al., 2018) *and Aspidosperma* (Alves et al., 2025) species have a well-developed, one-layered endothecium with fibrous thickening, although in *Oxypetalum appendiculatum*. Vital et al. (2015) found no evidence of endothecium thickening.

The characteristics of the tapetal cells described here indicate intense cellular activity; thus, they can be classified as secretory, similar to what has been reported for previously studied species of Apocynaceae (Alves et al., 2025). The importance of this tissue stems from its diverse roles in pollen grain development, including nourishing sporogenic tissue and microspores; synthesizing sporopollenin for pollen grain wall formation; producing orbicules (Ubisch bodies); secreting callose during tetrad formation; synthesizing and releasing substances, such as "pollenkitt" (lipids, flavonoids, and carotenoids), tryphine (a mixture of hydrophobic substances), enzymes, and recognition proteins, onto the pollen grain (Seale, 2020).

In the investigated *A. obesum* accession, tapetum degradation occurred early in young flower buds smaller than 1.5 cm in length and 0.2 cm in width, with sepals covering most of their length, well before the pre-anthesis stage.

Similarly, microsporogenesis in *A. obesum* occurs early, in young buds less than 1.0 cm in length and 0.15 cm in diameter. Microspores form through meiosis in buds smaller than 0.6 cm in length and 0.1 cm in width. Simultaneous cytokinesis was observed, resulting in tetrahedral tetrads, namely, a process also reported in other Apocynaceae, such as Rauvolfioids, Apocynoids and Periplocoideae, which may also exhibit the successive type (Endress et al., 2018). Simultaneous cytokinesis has also been observed in *Rauvolfia* (Ghimire et al., 2011; Koch et al., 2018) and *Aspidosperma* species (Alves et al., *2025*). In contrast, Vital and Nakamura (2018) reported that cytokinesis occurs successively in *O. appendiculatum*.

The entire microgametogenesis process occurred in young flower buds measuring 0.6 to 1.5 cm in length and 0.15 to 0.19 cm in width. The young microgametophyte formed after the degradation of the tapetum. Pollen grains completely developed in buds exceeding 1.5 cm in length and 0.2 cm in width, coinciding with the visible floral tube and sepals covering half the bud's length.

Although pollen grains are typically released in a three-celled stage in most members of the Apocynaceae family (Vital and Nakamura, 2018;

Alves et al., 2025), the samples analyzed here resemble those of *Rauvolfia vomitoria* and *R. weddelliana*, which show two-celled pollen grains in the dispersal stage (Koch et al., 2018). Thus, in *A. obesum*, the generative cell divides to produce male gametes only after the pollen tube has germinated.

In most Rauvolfioids and Apocynoids species, pollen grains are commonly released as monads; however, some taxa within these and other subfamilies release pollen in the form of tetrads (Endress, 2016; Endress et al., 2018). In *A. obesum*, although the pollen is dispersed as monads, the abundant lipidic substance surrounding the grains holds them together, enabling their mass dispersal and thereby facilitating pollination.

Angiosperms may disperse pollen with minimal starch content ('starchless') or, in some groups, with abundant starch reserves in the cytoplasm of the vegetative cell ('starchy') (Pacini and Dolferus, 2019). Our analyses indicate that pollen grains of *A. obesum* contain minimal starch at dispersal; thus, they are classified as starchless.

Interest in anther biology has considerably increased in recent decades owing to advances in genetic and molecular studies, their practical applications in plant breeding, and the growing demand for plant production.

Understanding the precise timing of the stages of microsporogenesis is crucial for reproductive aspects, family systematics, and has practical applications. Another culture, for example, could be an interesting alternative for improving *A. obesum*, as this method is suitable for cross-pollinating plants that require numerous crosses to obtain homozygous individuals. This technique is used in breeding programs for certain commercial species to accelerate the homozygosity process. To obtain double haploids, the flower bud stage must be identified when microspores form while still being enclosed in sporophytic tissues. Therefore, in this study, we recommend collecting samples classified between stages 2 and 3 to ensure that they are collected before the onset of microgametogenesis.

We also established morphological markers that relate androecium development events to easily visible characteristics in the buds and flowers of the species. This information can improve our understanding of the species by providing resources for family systematics, help characterize the reproductive performance of studied accessions, and establish a foundation for future in-vitro cultivation techniques aimed at the genetic improvement of *A. obesum*.

Conclusions

In this study, we characterized the androecium of *A. obesum*, documenting for the first time the anatomical structure of its gynostegium, as well as details of the development process of the parietal layers of the anther, microsporogenesis and megagametogenesis, and the characteristics of pollen grains at the dispersal stage. Additionally, we characterized the accession (ICA-pks), which showed no evidence of male sterility, suggesting its potential use as a pollen donor in experimental crosses.

Using easily observable morphological characteristics, collecting flower bud samples at pre-meiotic, meiotic, or post-meiotic developmental stages will be possible, contributing to the establishment of new protocols for in-vitro cultivation and plant breeding.

Acknowledgments

We would like to thank the Coordenação de Aperfeiçoamento de Pessoal de Nível Superior (CAPES) for the graduate scholarship, and Conselho Nacional de Desenvolvimento Científico e Tecnológico (CNPq) and Fundação de Amparo à Pesquisa do Estado de Minas Gerais (FAPEMIG) for the financial support granted for this study.

Author contribution

SN: Conceptualization, Formal Analysis, Investigation, financial, Writing – Review & Editing**. DCDC:** Investigation, Formal Analysis, Writing – Original Draft, Writing – Review & Editing. **CCFP:** Investigation, Visualization, Formal Analysis, Writing – Review & Editing. **EFAA:** Formal Analysis, Validation, Methodology, Writing – Review & Editing**. SMB:** Formal Analysis, Validation, Methodology, Writing – Review & Editing

Conflict of Interest

The authors declare that they have no known competing financial interests or personal relationships that could have appeared to influence the work reported in this paper.

Data Availability

Data will be made available upon request to the authors.

Declaration of generative AI and AI-assisted technologies in the writing process

The authors declare that the use of AI and AI-assisted technologies was not applied in the writing process.

References

ALVES, D.M.; SOUTO, L.S.; KOCH, I. Anther wall and pollen development in *Aspidosperma* Mart & Zucc. (Apocynaceae). **Botanical Journal of the Linnean Society**, v.207, p.70–82, 2025. https://doi.org/10.1093/botlinnean/boae033

BHANDARI, N.N. The microsporangium. In: **Embryology of Angiosperms**. JOHRI, B.M. (Ed.). Berlin/Heidelberg: Springer, 1984. p.53-121. https://doi.org/10.1007/978-3-642-69302-1_2

CARRILLO-OCAMPO, A.; ZAVALETA-MANCERA, H.A.; ENGLEMAN, E.M. Development of pollen grain and anther wall of *Tigridia pavonia* (L.F.) D.C. **Acta Microscopica**, v.32, n.2, p.16-28, 2023.

CHABAN, I.A.; KONONENKO, N.V.; GULEVICH, A.A.; BOGOUTDINOVA, L.R.N.; KHALILUEV, M.R.; BARANOVA, E.N. Morphological features of the anther development in tomato plants with non-specific male sterility. **Biology**, v.9, n.32, 2020. https://doi.org/10.3390/biology9020032

COLOMBO, R.C.; CRUZ, M.A.; CARVALHO, D.U.; HOSHINO, R. T.; ALVES, G.A.C.; FARIA, R.T. *Adenium obesum* as a new potted flower growth management. **Ornamental Horticulture**, v. 24, n.3, p.197-205, 2018. https://doi.org/10.14295/oh.v24i3.1226

COLOMBO, R.C.; FAVETTA, V.; YAMAMOTO, L.Y.; ALVES, G.A.C.; ABATI, J.; TAKAHASHI, L.S.A.; FARIA, R.T. Biometric description of fruits and seeds, germination and imbibition pattern of desert rose [*Adenium obesum* (Forssk.), Roem. & Schult.]. **Journal of Seed Science**, v.37, n.4, p.206-213, 2015. http://dx.doi.org/10.1590/2317-1545v37n4152811

ENDRESS, M.E.; MEVE, U.; MIDDLETON, D.J.; -SCHUMANN, S.L. Apocynaceae. In: KADEREIT, J.W.; BITTRICH, V. (eds). **Flowering Plants. Eudicots: Apiales, Gentianales (except Rubiaceae)**. Cham: Springer International Publishing, 2018. Vol XV. https://doi.org/10.1007/978-3-319-93605-5_3

ENDRESS, M.E.; BRUYNS, P.V. A revised classification of the Apocynaceae s.l. sl. **The Botanical Review**, v.66, n.1, p.1-56, 2000. https://doi.org/10.1007/BF02857781

ENDRESS, M.E.; LIEDE-SCHUMANN, S.; MEVE, U. An updated classification for Apocynaceae. **Phytotaxa**, v.159, n.3, p.175-194, 2014. http://dx.doi.org/10.11646/phytotaxa.159.3.2

ENDRESS, P.K. Development and evolution of the extreme synorganization in angiosperm flowers and diversity: a comparison of Apocynaceae and Orchidaceae. **Annals of Botany,** v.117, n.5, p.749-767, 2016. https://doi.org/10.1093/aob/mcv119

FALLEN, M.E. Floral structure in the Apocynaceae: morphological, functional, and evolutionary aspects. **Botanische Jahrbucher fur Systematik, Pflanzengeschichte und Pflanzengeographie**, v.106, p.245-286, 1986.

FISHBEIN, M.T.; LIVSHULTZ, S.C.K.; STRAUB, A.O.; SIMÕES, J.; BOUTTE, A., MCDONNELL, A.F. Evolution on the backbone: Apocynaceae phylogenomics and new perspectives on growth forms, flowers, and fruits. **American Journal of Botany,** v.105, n.3, p.495–513, 2018. https://doi.org/10.1002/ajb2.1067

GHIMIRE, B.; GHIMIRE, B.K.; HEO, K. Microsporogenesis in *Rauvolfia serpentina* (L.) Benth *ex* Kurz (Apocynaceae): an evidence for dual cytokinesis in microspore mother cells. **Journal of Medicinal Plants Research**, v.5, n.3, p.432-438, 2011.

HASTUTI, D.; SURANTO, S; SETYONO, P. V. Variation of morphology, karyotype and protein band pattern of adenium (*Adenium obesum*) varieties. **Nusantara Bioscience** [Indonesia], v.1, n.2, 2009. https://doi.org/10.13057/nusbiosci/n010205

JOHANSEN, D.A. **Plant microtechnique**. New York: Mcgraw-Hill Book, 1940. 523 p.

KOCH, I.; ALVES, D.M.; SOUTO, L.S. Anther wall and pollen development in two species of *Rauvolfia* L. (Apocynaceae). **Brazilian Journal of Botany**, v.41, n.1, p.175-184, 2018. https://doi.org/10.1007/s40415-017-0437-5

LASER, K.D.; LERSTEN, N.R. Anatomy and cytology of microsporogenesis in cytoplasmic male sterile angiosperms. **Botanical Review**, v.38, p.425-54, 1972.

NIETSCHE, S. Biology and structure of flowers in *Adenium obesum* (Forssk.) Roem. & Schult. (Apocynaceae) accessions with notes on the significance of these features for floriculture. **Brazilian Journal of Botany**, v.45, p. 689-702, 2022. https://doi.org/10.1007/s40415022-00804-5

NUNES, C.F.; PEREIRA, M.C.T. Produção de mudas e plantio de Rosa-do-deserto. In: NIETSCHE, S.; ALMEIDA, F.A.E.; MENDES, B.R. (eds.), **Cultivo e Manejo da Rosa-do-Deserto**. Brazilian Journals Publishing House, 2021. p.96-119.

O'BRIEN, T.P.; FEDER, N.; MCCULLY, M.E. Polychromatic staining of plant cell walls by toluidine blue O. **Protoplasma**, v.59, p.368-373, 1964. https://doi.org/10.1007/BF01248568

PACINI, E.; DOLFERUS, R. Pollen developmental arrest: maintaining pollen fertility in a world with a changing climate. **Frontiers in Plant Science**, v.10, 2019. https://doi.org/10.3389/fpls.2019.00679

PEREZ-LOPEZ, A.V.; LIM, S.D.; CUSHMAN, J.C. Humboldt Review: Tissue succulence in plants: Carrying water for climate change, **Journal of Plant Physiology**, v.289, 2023. https://doi.org/10.1016/j.jplph.2023.154081

PLAIZIER, A.C. A revision of *Adenium* Roem. and Schult. and of *Diplorhynchus* Welw. *ex* Fic. and Hiern (Apocynaceae). **Mededelingen Landbouwhoge School**, v.80, p.1-40, 1980.

POSSOBOM, F.C.C.; CANAVEZE, Y.; RAMOS, B.M.S. Aspectos Botânicos da Rosa-do-Deserto. In: NIETSCHE, S.; ALMEIDA, F.A.E.; MENDES, B.R. (eds.). **Cultivo e Manejo da Rosa-do-Deserto**. São José dos Pinhais: Brazilian Journals Publishing House, 2021. p.10-39.

RAMOS, S.M.B.; CARVALHO, M.A.S.; POSSOBOM, C.C.F.; ALMEIDA, E.F.A.; SANTOS, C.A.; LOUREIRO, G.A.H. DE A.; GOMES JÚNIOR, G.A.; PEREIRA, R.A.;SODRÉ, G.A.; BARBOSA, R.M. Seed germination and development of desert rose seedlings (*Adenium obesum* Roem. & Schult) on different substrates. **Ciência Rural**, v.50, n.12, 2020. https://doi.org/10.1590/0103-8478cr20190691

SANTOS, M.M.; COSTA, R.B.; CUNHA, P.P.; SELEGUINI, A. Tecnologias para produção de mudas de rosa do deserto (*Adenium obesum*). **Multi-Science Journal**, v.1, n.3, p.79-82, 2015. https://doi.org/10.33837/msj.v1i3.124

SEALE, M. Callose deposition during pollen development. **Plant Physiology**, v.184, n.2, p.564-565, 2020. https://doi.org/10.1104/pp.20.01143

SEGUÍ-SIMARRO, J.M. Doubled haploid technology. **Emerging Tools, Cucurbits, Trees, Other Species**, Humana Press. 2021. 338p. vol 3.

SIMÕES, A.O.; RIO, M.C.S.; CASTRO, M.M.; KINOSHITAY, L.S. Gynostegium morphology of *Mesechiteae miers* (Apocynaceae, Apocynoideae) as it pertains to the classification of the tribe. **International Journal of Plant Science**, v.168, n.7, 999-1012, 2007.

SINGH, A.; CHAVAN, S.; BHANDARI, A.J.; PAREKH, V.; SHAH, H.P.; PATEL, B.N. New Multipetalous Variety G. Ad.1 of Adenium obesum. **International Journal of Current Microbiology and Applied Sciences**, v.8, n.7, p.197-203, 2019. https://doi.org/10.20546/ijcmas.2019.807.025

SOLOMON RAJU, A.J.; SUNANDA DEVI, D.; VENKATA RAMANA, K.; PUNNY, K. Sexual system, pollination mechanism, pollinators and seed dispersal in some species of the sub-families, Asclepiadoideae and Rauvolfioideae of the family Apocynaceae. **Species**, v.22, n.69, p.97-117, 2021.

SOUZA, C.G.; RAMOS, S.M.B.; NIETSCHE, S.; POSSOBOM, C.C.F.; ALMEIDA, E.F.A.; PEREIRA, M.C.T. Viability of pollen grains and stigma receptivity in Desert Rose. **Ornamental Horticulture**, v.28, n.1, p.92-98, 2022. https://doi.org/10.1590/2447-536X.v28i1.2402

SUD, K.C. A contribution to the embryology of *Trachelospermum fragrans* Hook. f. (Apocynaceae). **Proceedings Indian Academy Plant Science**, v.93, p.495-501, 1984. https://doi.org/10.1007/BF03053215

VITAL, F.A.Z.; NAKAMURA, A.T. Androecium development of *Oxypetalum appendiculatum* Mart. (Apocynaceae): A Taxonomic Approach. **Scientific Electronic Archives**, v.11, n.5, p.130-139, 2018. https://doi.org/10.36560/1152018739